sciendo

QPI 2020, volume 2, pp. 247-258

MECHANICAL PROPERTIES THE Al-7%SiMg ALLOY WITH CuAl10Fe3Mn2 USED IN MACHINE BUILDING AND CIVIL ENGINEERING

doi: 10.2478/cqpi-2020-0028

Date of submission of the article to the Editor: 12/08/2020
Date of acceptance of the article by the Editor: 03/09/2020

Tomasz Lipiński – *orcid id: 0000-0002-1644-1308*
University of Warmia and Mazury in Olsztyn, **Poland**

Abstract: Silumins are one of the most popular group among aluminum casting alloys. They are characterized by good mechanical and casting properties, low density, good electric and thermal conductivity, a low degree of contraction, good corrosion resistance and a relatively low melting temperature.
The mechanical properties of hypoeutectic silumins can be improved through chemical modification as well as traditional or technological processing. Modification improves the mechanical properties of alloys through grain refinement. The effect of treatment has been given a lot of information first of all about microstructure and mechanical properties. This study presents the results of treatment of an Al-7%SiMg alloy with composition CuAl10Fe3Mn2 (as a powder) + (Al-7%SiMg + CuAl10Fe3Mn2) (as a powder) + (Al-7%SiMg + CuAl10Fe3Mn2) (in the form of a rod) in three different ranges. The experiments were conducted following a factor design 2^3 for 3 independent variables. The main addition was aluminum bronze, as well as clear or melted with raw alloy. The influence of the analyzed modifiers on the microstructure and mechanical properties of the processed alloy was presented in graphs. The modification of a hypoeutectic Al-7%SiMg alloy improved the alloy's properties. The results of the tests indicate that the mechanical properties of the modified alloy are determined by the components introduced to the alloy.

Keywords: Al-Si alloys, aluminum bronze, mechanical properties

1. INTRODUCTION

Hypoeutectic Al-7%SiMg alloy is one of the most popular casting Al-Si alloys. They are characterized by good mechanical and founding properties, low density, good electric and thermal conductivity, a low degree of contraction low price, good corrosion resistance and high tensile strength with low specific gravity, a relatively low low melting point and first of all easy to carry out the casting process. In hypoeutectic alloys of aluminum and silicon, solid solution dendrites which crystallize first are typical crystals, showing isotropic properties. Similarly to pure aluminum, large well deformable alpha phase solid solution α (silicon in aluminum) has a regular cubic face-centered lattice of the type A1. The growth rate of those crystals, and the growth rate of eutectic mixture

crystallizing at the next stage (α+β) with sharp-pointed hard, non-deformable β-phase, is a function of supercooling at the crystallization front. This dependence is a complex function of the chemical composition, of the liquid and solid phase, surface curvature of the crystallization front, crystallization, heat emission structural defects and many more. The mechanical properties of hypoeutectic silumins are affected by size the α-phase and mainly the shape and size of eutectic mixture (α+β). These unmodified phases of microstructure composition give the alloy a low tensile strength and elongation close to zero. This is the reason for not using alloy in this form (Michna et al., 1991), (Braszczyński, 1991), (Vaněček et al., 2003), (Mondelfo, 1976), (Bolibruchová, Richtárech, 2016), (Góral et al., 2006), (Kusmierczak et al., 2017). In the Al-Si-Cu equilibrium system (Fig. 1), apart from the typical phases for the Al-Si alloy (α and β), there is also Al_2Cu.

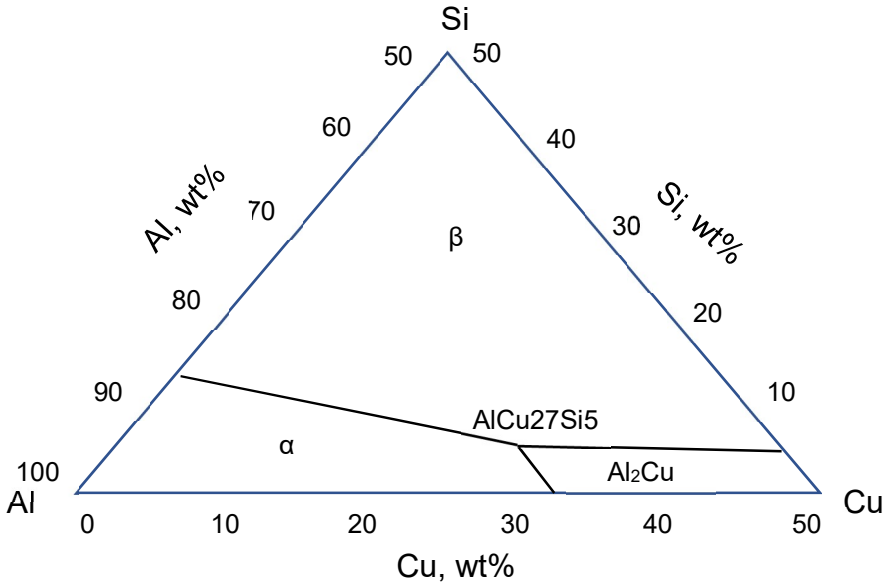

Fig. 1. Scheme of diagram of the Al-Si-Cu system (Ruan, Wei, 2009), (Raghavan, 2010), (Villars et al., 1995)

Reducing the weight of the working machines is able in the position improve performance and reduced fuel consumption and exhaust emissions. This can be achieved by optimizing the construction and use of light materials. It is the reason why aluminum is growing in popularity, mainly in the automotive industry and working machines, including agriculture. Suppliers for the automotive industry are constantly forced to design such materials, which not only ensures higher and higher properties, but also reduce the negative impact on the environment. In the case of materials used in construction (e.g. window frames, facade elements), not only the strength parameters and corrosion resistance are important, but also the mass of the building.

The microstructure and closely related with it properties Al-7%SiMg silumin and other alloys requires quality control and a changed (Ulewicz et al., 2016), (Borkowski et al. 2012), (Wojnar et al., 2016). These changes can be implemented, depending on the type of alloy through technological processes (Bruna, Sladek, 2016), (Pilarczyk, 2015), (Nová, Machuta, 2013), (Vitalii, Dudek, 2017), (Stasiak-Betlejewska, Ulewicz, 2016), (Styrylska, 1992) through solidification processes (Wołczyński, 2012), (Vandersluis, 2018), (Fisher, Kurz, 1977), modification and treatment chemical elements (Náprstková et al., 2013), (Lipiński, 2010), (Lipinski, Szabracki, 2013), (Bolibruchová, Richtárech,

2013), (Lipinski, 2015b), (Novák et al.), (Lipiński, 2008a), (Cook, 2008) or processing (Wołczyński et al. 2017), (Hajek et al., 2015), (Dudek, Lisiecka, 2017), (Ulewicz et al., 2013), (Hao et al., 2011), (Osorio et al., 2008). In the majority of cases alloys are modified to change the form and size of grains, mostly silicon grains, which reduces the interphase spacing of eutectic (α+β) and reducing the size of the primary alpha phase, but first of all large beta phase (Michna et al., 2005), (Mondelfo, 1976). The researches indicate that the reaction's thermal effects as a solidification process affects the result of the modification process, what causes to changes in the size and shape of alloy phases and obtaining the expected properties of the alloy (Mondelfo, 1976), (Náprstková et al., 2014).

There are another interesting effective modern methods ecological modification by the use of homogenous modifiers (Lipiński, 2008a, 2010), as well as exothermic modifiers that produce exothermic effects in the modification process of alloys (Lipiński, 2008b, 2011), (Bolibruchová, Richtárech, 2013). Modification with exothermic modificator allows you to enter the chemical elements into the liquid alloy. The chemical elements introduced not only improve the microstructure of the treated alloy but also increase its performance characteristics. Silumin modification with modifiers composed of several components (mixtures) is more effective that modification with individual alloy-forming elements. The strontium effect is described in the literature by modifying eutectics (Michna et al., 2005), (Náprstková et al., 2013), (Lipiński, 2015a).

The results of studies on the change of microstructure of hypoeutectic aluminum-silicon liquid alloys mainly with sodium and strontium and other chemical elements and mixtures have already been tested and published and described by many authors (Cook, 2008), (Lipiński, 2015b). However, it should be remembered that there are a lot of research for improvement mechanical properties by technological methods, too (Nová, Machuta, 2013), (Fisher, Kurz, 1977) (Lipiński, 2015c). However, widely presented books and research papers on the silumin treatment give not a lot of contents on the effect treatment with aluminum bronze (Chrostek, 2016). In view of the high popularity of Al-7% SiMg alloys the purpose of the study was to determine the mechanical properties of hypo-eutectic silumin Al-7% SiMg modified with CuAl10Fe3Mn2 (as a powder) + (Al-7%SiMg + CuAl10Fe3Mn2) (as a powder) + (Al-7%SiMg + CuAl10Fe3Mn2) (in the form of a rod) added in different range of components.

2. MATERIALS AND METHODS

The experiment performed on Al-7%SiMg hypoeutectic alloy, produced industrially and supply in the pig sows. The chemical composition of the raw Al-7%SiMg alloy is presented in Table 1.

Table 1
Chemical composition of the tested Al-7%SiMg alloy

Chemical composition, wt. %									
Si	Cu	Mg	Mn	Fe	Ti	Ni	Zn	Pb	Al
7.2	0.10	0.10	0.30	0.20	0.10	0.03	0.15	0.07	ball

The alloy was melted in a ceramic cruciblein an laboratory electric furnace Nabertherm 30 – 3000. The treatment process was performed with CuAl10Fe3Mn2 and Al-7%SiMg

alloy. Mixtures CuAl10Fe3Mn2 and Al-7%SiMg has 50% CuAl10Fe3Mn2 + 50% Al-7%SiMg alloy. After remelting, the mixture was casted into 3.5 mm diameter rods or crushed to a 0.35 to 0.50 mm fraction. The alloy with addition elements was melted at 850°C for 8 minutes. Dry sand molds formed in the shape of a cylinder of 75 mm in length and 8 mm in diameter was filled with the liquid Al-7%SiMg alloy with modifier. From each casting two specimens were obtained. Brinell method was determined hardness by using a test force value of 612.9 N, ball diameter of 2.5 mm, force-diameter index was 10 and duration time of test force 20 s. Hardness was measured on side surface of the head of the test pieces prepared to tensile test prepared by grinding to a depth of 2 mm. Three hardness measured per sample (6 measurements per cast) were made. All Brinell hardness measurements were performance according to standard PN EN ISO 6506-1:2014 in the HPO 250 hardness tester. The tensile stress test was carried out on a test pieces with ratio of 1:5 (a diameter-to-length) by used the ZD-30j universal tensile tester to determine ultimate tensile strength and percentage elongation. A tensile strength and elongation test was carried out on two ϕ 6 mm sample for each research points, according to standard PN EN ISO 6892-1:2016. The experiments was conducted by a factor plan 2^3 for three independent variables. Variable and its levels is presented in Table 2. The regression equation for each research parameter was presented as (1).

$$\hat{y} = b_0 + b_1x_1 + b_2x_2 + b_3x_3 + b_{12}x_1x_2 + b_{13}x_1x_3 + b_{23}x_2x_3 + b_{123}x_1x_2x_3 \quad (1)$$

Table 2
Level of variables

Variable	Primary level, %	Range of changes, %	Higher level, %	Lower level, %
CuAl10Fe3Mn2 (as a powder)	3	1	4	2
(Al-7%SiMg + CuAl10Fe3Mn2) (as a powder)	3	1	4	2
(Al-7%SiMg + CuAl10Fe3Mn2) (in the form of a rod)	3	1	4	2

The results have been subjected to statistical analysis at the level of significance α = 0.05. The adequacy of the regression equation was verified by means of the Fischer criterion for p=0.05.

Before corrosion experiments, the test of pieces with an area of 24 cm^2 (40 x 10 x 10 mm) were successively polished with emery paper to about Ra = 0.25 μm, next cleaned with 95% alcohol. The samples AlSi7Mg with 4% (Al-7%SiMg + CuAl10Fe3Mn2) (as a powder) + 2% (Al-7%SiMg + CuAl10Fe3Mn2) (in the form of a rod) + 2% Al10Fe3Mn2 (as a powder) was tested accordance to standard dedicated for stainless steel PN EN ISO 3651-1. Corrosion test in 1% HCl water solution medium was tested by measurement of loss in mass.

The corrosion rate of the tested alloy measured in mm/year was calculated with the formula (1), but measured in g/m2 were calculated with the below formula (2):

$$r_{corm}=(87600\cdot m)/(S\cdot t\cdot \rho) \quad (1)$$

$$r_{corg}=(10000\cdot m)/(S\cdot t) \quad (2)$$

where:
t – time of corrosion test (for each sample counted from zero), hours,
S - surface area of the sample, cm^2,
m – average mass loss in corrosion process, g,
ρ - sample density, g/cm^3.

The influence of 1% HCl on corrosion resistance was investigated using weight loss. The mass of samples were measured by Kern ALT 3104AM general laboratory precision balance with accuracy of measurement 0.0001 g. Every with measurements was repeated five times.
Profile roughness parameters was analyzed according to the PN-EN 10049:2014-03 standard (Measurement of roughness average Ra and peak count RPc on metallic flat products) by the Diavite DH5 profilometer.

2. RESULTS AND DISCUSSION

Results of the ultimate tensile strength (UTS) of Al-7%SiMg alloy with mixtures (1) is shown at Fig. 2, elongation (A) at Fig. 3 and Brinell hardness (HB) at Fig. 4. Due to difficulties with representing functions for three independent variables, figure drawings for the obtained function were developed from the experimental design on the assumption that each of the analyzed modifier components was present at a stable higher (2%) or lower (1%) level while the share of the remaining two components varied. Based on this approach, six graphic forms were developed and two presented (Figs. 2-4) for three modifier components. For an raw Al-7%SiMg alloy, average ultimate tensile strength for three test pieces was defined at UTS = 139 MPa, elongation A=0,2% and Brinell hardness H=47 HB. After treatment tested based silumin by 2% (Al-7%SiMg + CuAl10Fe3Mn2) (as a powder) + 2% (Al-7%SiMg + CuAl10Fe3Mn2) (in the form of a rod) + 2% Al10Fe3Mn2 (as a powder) ultimate tensile strength was increased to 165 MPa (Fig. 2b), elongation to 0.3% (Fig. 3b) and Brinell hardness to 48 (Fig. 4b). For increased mixture (Al-7%SiMg + CuAl10Fe3Mn2) (as a powder) to 4% the UTS=179 MPa (Fig 2b) elongation to 2.6% (Fig. 3b) and Brinell hardness to 56 (Fig. 4b). There are the maximal values. In the similar way can be analyzed all research points and figures.
At constant Sr content the highest effective influence mixture was observed for the (Al-7%SiMg + CuAl10Fe3Mn2) (as a powder) at a higher level. The effect of Al-7%SiMg with CuAl10Fe3Mn2 as a powder was found to be more effective than Al-7%SiMg with CuAl10Fe3Mn2 as a rod. Since all analyzed properties of the treatment alloy are higher after treatment with the mixture of aluminum bronze and the native alloy than with the same aluminum bronze (Figs 2, 3, 4), it should be concluded that the mixture in the form of a mortar with a native alloy interacts more effectively.

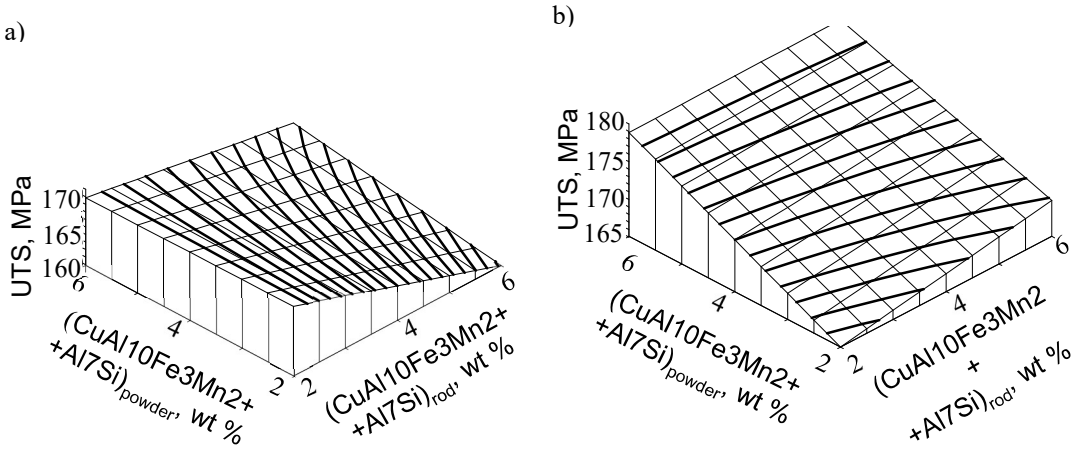

Fig. 2. The ultimate tensile strength (UTS) Al-7%SiMg alloy with: (Al-7%SiMg + CuAl10Fe3Mn2) (as a powder) ∈<2, 4> % and (Al-7%SiMg + CuAl10Fe3Mn2) (in the form of a rod) ∈<2, 4> % for a) CuAl10Fe3Mn2 (as a powder) = 1%; b) CuAl10Fe3Mn2 (as a powder) = 2%

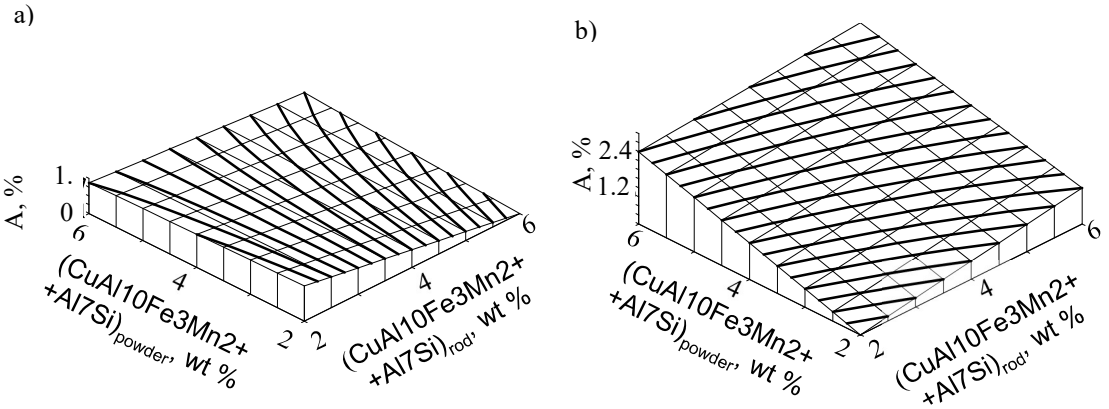

Fig. 3. Elongation (A) Al-7%SiMg alloy with: (Al-7%SiMg + CuAl10Fe3Mn2) (as a powder) ∈<2, 4> % and (Al-7%SiMg + CuAl10Fe3Mn2) (in the form of a rod) ∈<2, 4> % for a) CuAl10Fe3Mn2 (as a powder) = 1%; b) CuAl10Fe3Mn2 (as a powder) = 2%

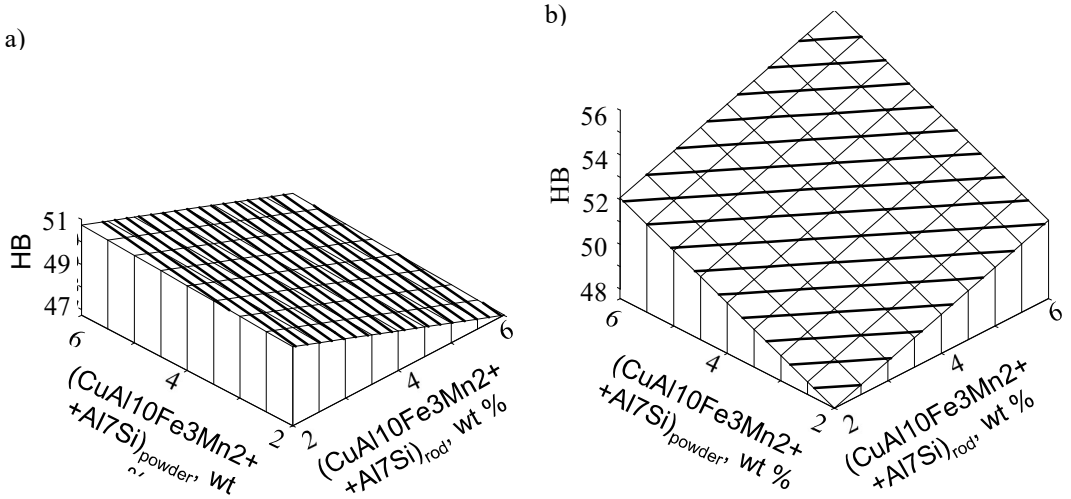

Fig. 4. Brinell hardness (HB) Al-7%SiMg alloy with: (Al-7%SiMg + CuAl10Fe3Mn2) (as a powder) ∈<2, 4> % and (Al-7%SiMg + CuAl10Fe3Mn2) (in the form of a rod) ∈<2, 4> % for a) CuAl10Fe3Mn2 (as a powder) = 1%; b) CuAl10Fe3Mn2 (as a powder) = 2%

Microstructure of Al-7%SiMg alloy with 2% (Al-7%SiMg + CuAl10Fe3Mn2) (as a powder) + 2% (Al-7%SiMg + CuAl10Fe3Mn2) (in the form of a rod) + 4% Al10Fe3Mn2 (as a powder) (the best mechanical properties)is presented in Fig. 5. The a little refinement of primary dendrites of β phase was observed after all the processing of the Al-7%SiMg alloy in accordance to investigation plane (tab. 2). Analyzing the microstructure of both alloys was noted in both variants the likely occurrence of the grey needle-granular eutectic β phase and grains white α phase, on a dark background eutectoid α + γ2 and dark precipitates of Chinese writings. Also can be observed individually occurring separation of κ phase.

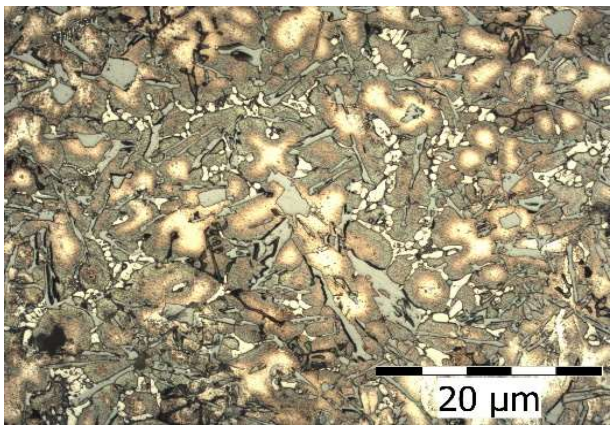

Fig. 5. Microstructure of AlSi7Mg alloy with: 2% (Al-7%SiMg + CuAl10Fe3Mn2) (as a powder) + 2% (Al-7%SiMg + CuAl10Fe3Mn2) (in the form of a rod) + 4% Al10Fe3Mn2 (as a powder).

Exemplary profile roughness of AlSi7Mg alloy with: 2% (Al-7%SiMg + CuAl10Fe3Mn2) (as a powder) + 2% (Al-7%SiMg + CuAl10Fe3Mn2) (in the form of a rod) + 4% Al10Fe3Mn2 (as a powder) after corrosion tests 1% HCl at room temperature and time 336 and 432 hours is presented in Fig. 6 and 7.

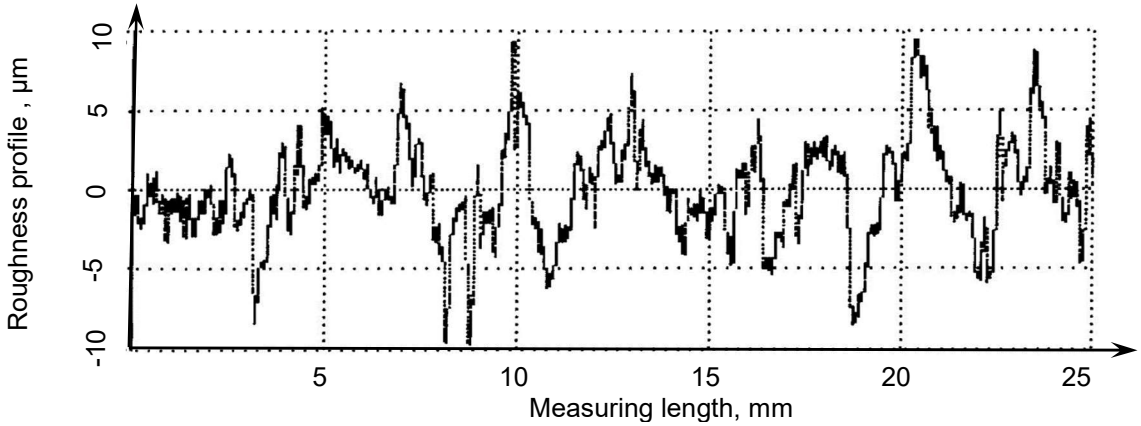

Fig. 6. Profile roughness of AlSi7Mg alloy width (R_q) of AlSi7Mg alloy with 4% (Al-7%SiMg + CuAl10Fe3Mn2) + 2% (Al-7%SiMg + CuAl10Fe3Mn2) + 2% Al10Fe3Mn2 after corrosion tests 1% HCl at room temperature and time 336 hours.

Maximum peak height (Rp) value and total height of the roughness profile (Rt) value of AlSi7Mg alloy with 4% (Al-7%SiMg + CuAl10Fe3Mn2) + 2% (Al-7%SiMg + CuAl10Fe3Mn2) + 2% Al10Fe3Mn2 after corrosion tests in 1% HCl at room temperature is presented in Fig. 8.

Maximum peak height (Rp) value and total height of the roughness profile (Rt) value of AlSi7Mg alloy with 4% (Al-7%SiMg + CuAl10Fe3Mn2) + 2% (Al-7%SiMg + CuAl10Fe3Mn2) + 2% Al10Fe3Mn2 after corrosion tests in 1% HCl at room temperature is presented in Fig. 9.

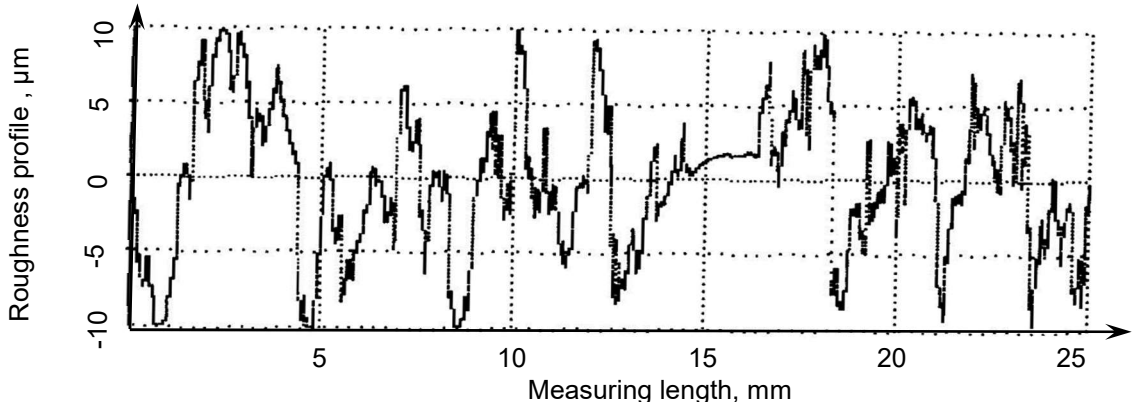

Fig. 7. Profile roughness of AlSi7Mg alloy width (R_q) of AlSi7Mg alloy with 4% (Al-7%SiMg + CuAl10Fe3Mn2) + 2% (Al-7%SiMg + CuAl10Fe3Mn2) + 2% Al10Fe3Mn2 after corrosion tests 1% HCl at room temperature and time 432 hours.

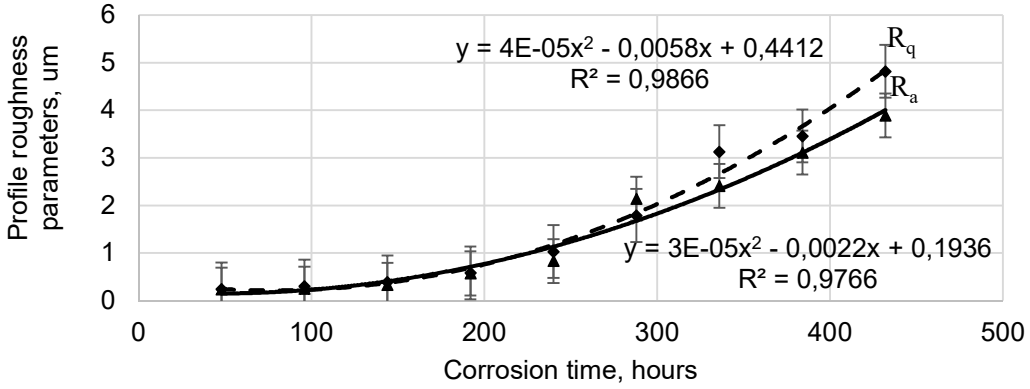

Fig. 8. Arithmetical mean roughness (R_a) value and mean peak width (R_q) of AlSi7Mg alloy with 4% (Al-7%SiMg + CuAl10Fe3Mn2) + 2% (Al-7%SiMg + CuAl10Fe3Mn2) + 2% Al10Fe3Mn2 after corrosion tests 1% HCl at room temperature

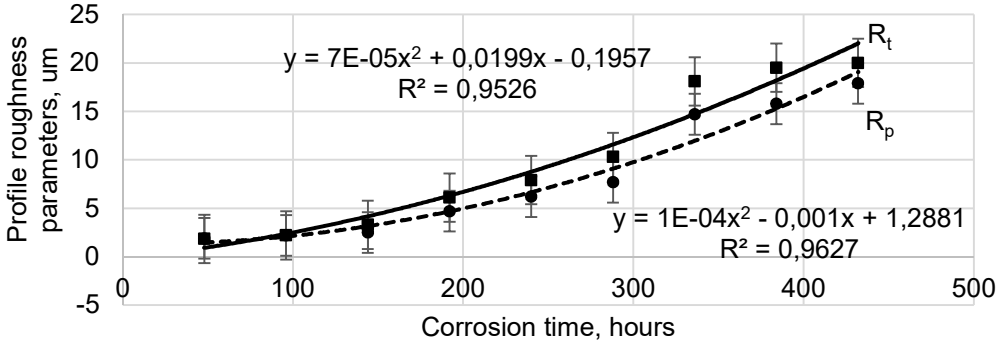

Fig. 9. Maximum peak height (Rp) value and total height of the roughness profile (Rt) value of AlSi7Mg alloy with 4% (Al-7%SiMg + CuAl10Fe3Mn2) + 2% (Al-7%SiMg + CuAl10Fe3Mn2) + 2% Al10Fe3Mn2 after corrosion tests in 1% HCl at room temperature.

Effects of corrosion time on the relative mass loss (RML) of AlSi7Mg alloy with 4% (Al-7%SiMg + CuAl10Fe3Mn2) + 2% (Al-7%SiMg + CuAl10Fe3Mn2) + 2% Al10Fe3Mn2 after corrosion tests in 1% HCl at room temperature is presented in Fig. 10.
Effects of corrosion time on on the corrosion rat rcorm (mm/year) of AlSi7Mg alloy with 4% (Al-7%SiMg + CuAl10Fe3Mn2) + 2% (Al-7%SiMg + CuAl10Fe3Mn2) + 2% Al10Fe3Mn2 after corrosion tests in 1% HCl at room temperature is presented in Fig. 11.

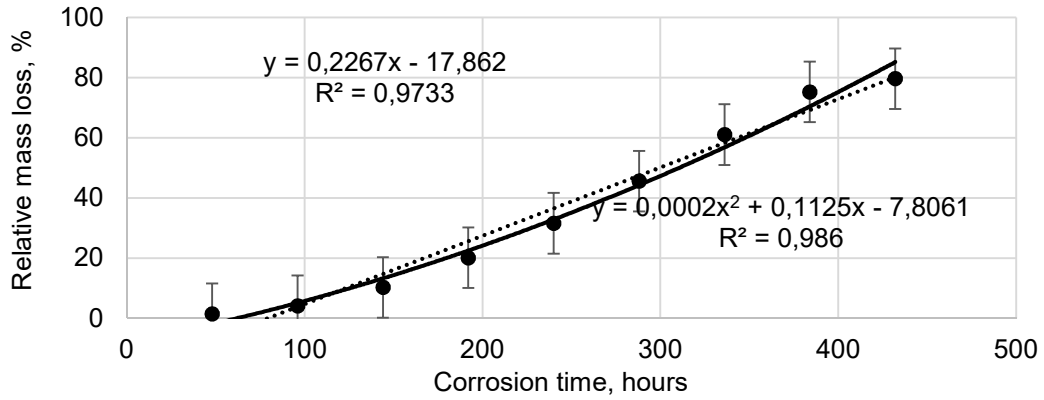

Fig. 10. Effects of corrosion time on the relative mass loss (RML) of AlSi7Mg alloy with 4% (Al-7%SiMg + CuAl10Fe3Mn2) + 2% (Al-7%SiMg + CuAl10Fe3Mn2) + 2% Al10Fe3Mn2 after corrosion tests in 1% HCl at room temperature.

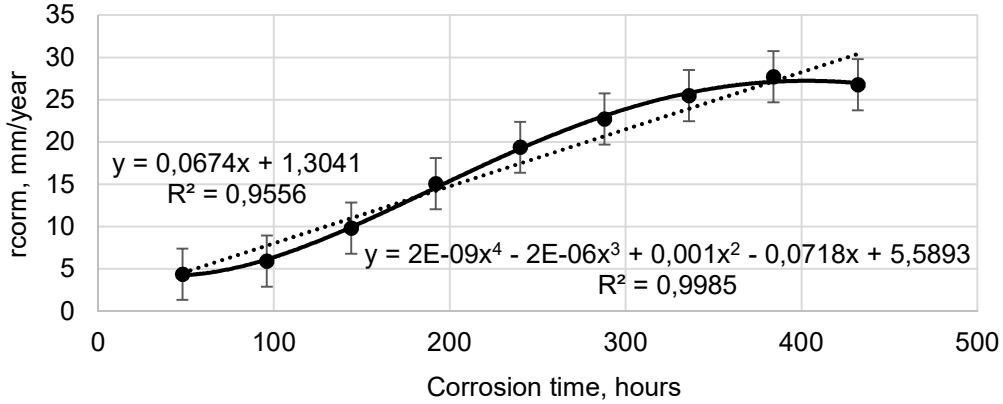

Fig. 11. Effects of corrosion time on on the corrosion rate r_{corm} (mm/year) of AlSi7Mg alloy with 4% (Al-7%SiMg + CuAl10Fe3Mn2) + 2% (Al-7%SiMg + CuAl10Fe3Mn2) + 2% Al10Fe3Mn2 after corrosion tests in 1% HCl at room temperature.

Effects of corrosion time on on the corrosion rat r_{corm} (g/m^2) of AlSi7Mg alloy with 4% (Al-7%SiMg + CuAl10Fe3Mn2) + 2% (Al-7%SiMg + CuAl10Fe3Mn2) + 2% Al10Fe3Mn2 after corrosion tests in 1% HCl at room temperature is presented in Fig. 12.
During the first 96 h of soaking AlSi7Mg alloy with 4% (Al-7%SiMg + CuAl10Fe3Mn2) + 2% (Al-7%SiMg + CuAl10Fe3Mn2) + 2% Al10Fe3Mn2 in 1% HCl, the roughness parameters R_a, R_q, R_t and R_p increased by a few percent. After lengthening the soaking time, a faster increase in the size of these parameters was observed, the distribution of which with a statistical accuracy of over 95% was described by a second-degree exponential curve (Figs. 8 and 9). A similar distribution was found for relative mass loss (Fig. 10) and corrosion rate (Fig. 11 and 12). The gradual flattening of the corrosion rate charts (Fig. 11 and 12), indicating a decrease in the corrosion rate, is most likely caused

by a gradual reduction in the surface of the impact of an aggressive environment resulting from the decreasing active surface of the sample in the corrosion wear skins.

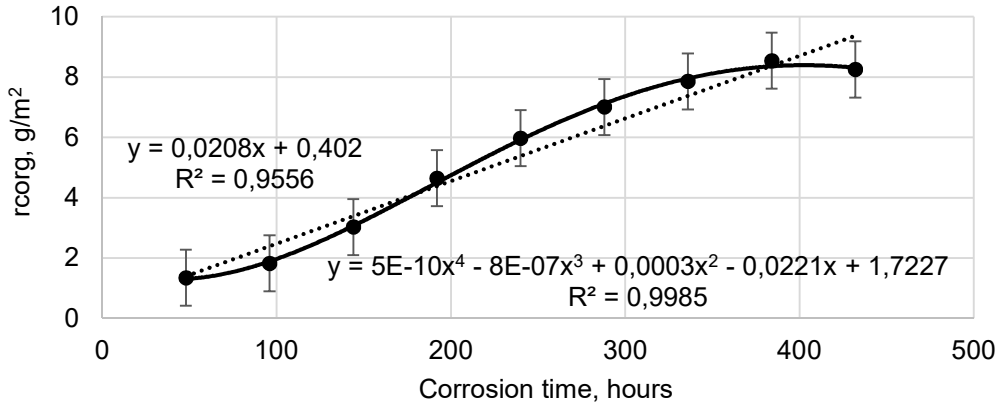

Fig. 12. Effects of corrosion time on on the corrosion rate r_{corm} (g/m^2) of AlSi7Mg alloy with 4% (Al-7%SiMg + CuAl10Fe3Mn2) + 2% (Al-7%SiMg + CuAl10Fe3Mn2) + 2% Al10Fe3Mn2 after corrosion tests in 1% HCl at room temperature.

3. CONCLUSION

1. Results of the research showed the possibility of introducing CuAl10Fe3Mn2 addition to the Al-7% SiMg alloy both in native form and in the form of mortar made with a treatment alloy.
2. The best results were obtained for a treatment Al-7%SiMg alloy with 4% (Al-7%SiMg + CuAl10Fe3Mn2) (as a powder) + 2% (Al-7%SiMg + CuAl10Fe3Mn2) (in the form of a rod) + 2% Al10Fe3Mn2 (as a powder), which enabled to achieve the highest values of all analyzing parameters (in this experimental plan).
3. The alloy obtained by remelting silumin and aluminum bronze due to phase inheritance of both alloys can be an interesting composition and is worth further analysis in terms of its applicability.
4. Analyzing the course of changes in roughness, it was found that its description of the function of the first degree is statistically adequate and has a high degree of fit (r^2>0.95).
5. The obtained roughness curves in the first corrosion period are proportional. In the second period of corrosion, there was more and more roughness in each subsequent unit of time. For this reason, the description of the curves of the roughness as a function of the second degree is more accurate.
6. Counted from zero time of corrosion test showed a reduction in corrosion rate. In this way based on the graph or equation it is possible to estimate total corrosion rate at any time, counted from the beginning of the corrosion measurement.
7. By using equations describing material roughness or corrosion rate, it is possible to determine conditions for automatic control of the condition of an object.

LITERATURE

Bolibruchová, D., Richtárech, L., 2013. Effect of adding iron to the AlSi7Mg0.3 (EN AC 42 100,A356) alloy. Manufacturing Technology 13(3), 276-281.

Bolibruchová, D., Richtárech, L., 2016, Possibilities of Using Al-Si-Mg Alloys with Higher Fe Content for Demanding Castings. Manufacturing Technology 16(2), 317-323.

Borkowski, S., Ulewicz, R., Selejdak, J., Konstanciak, M., Klimecka-Tatar, D., 2012. The use of 3x3 matrix to evaluation of ribbed wire manufacturing technology. 21st Int. Conf. on Metallurgy and Materials. Ostrava: TANGER, 1722-1728.

Braszczyński J., 1991, Krystalizacja odlewów. WNT Warszawa.

Bruna, M., Sládek, A., 2016, Hot Tearing Evaluation of Al Based Alloys. Manufacturing Technology 16(2), 323-327.

Chrostek, T., 2016. Thermalanalysis of aluminum bronze BA1032. Technical Sciences 19(4), 359–366.

Cook, R., 2008. Modification of Aluminium-Silicon Foundry Alloys. London & Scandinavian Metallurgical Co Limited.

Dudek, A., Lisiecka, B., 2017. The effect of thermal oxidation of porous and non-porous titanium alloy. Metal 2017: 26th International Conference on Metallurgy and Materials. TANGER Ltd 1234-1239.

EN ISO 6892-1:2016. Metallic materials. Tensile testing Part 1: Method of test at room temperature.

EN ISO6506-1:2014. Metallic materials -- Brinell hardness test Part 1: Test method.

Fisher, D.J., Kurz, W., 1977. Coupled zones in faced/nonfaced eutectics. Solidification and casting of metals. International conference on solidification. Sheffield.

Góral, A., Jura, J., Bouzy, E., Sztwiertnia, K., Morgiel, J., Bonarski, J., 2006. Multiscale texture and orientation relationship investigation in Al-CuAl2 eutectic alloy, Archives of Metallurgy and Materials 51, 11-14.

Hajek, J., Kriz, A., Hrydlicka, V., 2015. The heat treatment of aluminium bronzes. Manufacturing Technology 15(1), 35-41.

Hao, Y., Gao, B., Tu, G.F., Li, S.W., Hao, S.Z., Dong, C., 2011. Surface modification of Al–20Si alloy by high current pulsed electron beam. Applied Surface Science 257, 3913–3919.

Kusmierczak, S., Müller, M. Lebedev, A., 2017. Evaluation of aluminium alloy surface machined by means of abrasive-free ultrasonic finishing. In 16th International Scientific Conference: Engineering For Rural Development 24.05.2017, Latvia Univ Agriculture, Faculty Engineering 167-174.

Lipiński, T., 2008. Modification of Al-Si alloys with the use of a homogenous modifiers. Archives of Metallurgy and Materials 53(1), 193-197.

Lipiński, T., 2008. Influence exothermical mixtures contents Na or B on elongation and hardness AlSi12 alloy. Archives of Foundry Engineering 8(1), 81-84.

Lipiński, T., 2010. The structure and mechanical properties of Al-7%SiMg alloy treated with a homogeneous modifier. Solid State Phenomena 163, 183-186.

Lipiński, T., 2011. Use Properties of the AlSi9Mg Alloy with Exothermical Modifier. Manufacturing Technology 11(11), 44-49.

Lipinski, T., 2015. Double modification of AlSi9Mg alloy with boron, titanium and strontium. Archives of Metallurgy and Materials 60(3), 2415-2419.

Lipiński, T., 2015. Modification of Al-11% Si Alloy with Cl – Based Modifier. Manufacturing Technology 15(4), 581-587.

Lipiński, T., 2015. Influence of Surface Refinement on Microstructure of Al-Si Cast Alloys Processed by Welding Method. Manufacturing Technology 15(4), 576-581,

Lipinski, T., Szabracki, P., 2013. Modification of the Hypo-Eutectic Al-Si Alloys with an Exothermic Modifier. Archives of Metallurgy and Materials 58(2), 453-458.

Michna, S., Lukac, I., Ocenasek, V., Koreny, R., Drapala, J., Schneider, H., Miskufova, A., 2005. Encyclopaedia of aluminium, Adin s.r.o. Presov. (in Czech).

Mondelfo, L.F., 1976. Aluminium alloys. Structure and properties. Butter Wooths. London Boston.

Náprstková, N., Cais, J., Stančeková, D., 2014. Influence of Alsi7Mg0.3 Alloy Modification by Sb on the Tool Wear. Manufacturing Technology 14(1), 75-79

Náprstková, N., Kuśmierczak, S., Cais, J., 2013. Modification of AlSi7Mg0.3 alloy by strontium. Manufacturing Technology 13(3), 373-380.

Nová, I., Machuta, J., 2013. Squeeze casting results of aluminium alloys. Manufacturing Technology 13(1), 73-79.

Novák, P., Šerák, J., Vojtěch, D., Zelinková, M., Mejzlíková, L., Michalcová, A., 2011. Effect of Alloying Elements on Microstructure and Properties of Fe-Al and Fe-Al-Si Alloys Produced by Reactive Sintering. Key Engineering Materials 465, 407-410.

Osorio, W.R., Cheung, N., Spinelli, J.E., Cruz, K.S., Garcia, A., 2008. Microstructural modification by laser surface remelting and its effect on the corrosion resistance of an Al–9 wt%Si casting alloy. Applied Surface Science 254, 2763–2770.

Pilarczyk, W., 2015. The investigation of the structure of bulk metallic glasses before and after laser welding. Cryst. Res. Technol. 9-10, 700-704.

PN EN ISO 3651-1, Determination of resistance to intergranular corrosion of stainless steels. Part 1: Austenitic and ferritic-austenitic (duplex) stainless steels.

Raghavan, V., 2010. Al-Cu-Si (Aluminum-Copper-Silicon). J. Phase Equilib. Diffus. 31, 39–40.

Ruan, Y., Wei, B.B., 2009. Rapid solidification of undercooled Al-Cu-Si eutectic alloys. Chinese Sci. Bull. 54, 53–58.

Stasiak-Betlejewska, R., Ulewicz, R., 2016. The effectiveness of selected machinery and equipment in the woodworking joinery. Path forward for wood products: a global perspective, proceedings of scientific papers 149-156.

Styrylska, T., Pietraszek, J., 1992. Numerical modeling of non-steady-state temperature fields with supplementary data. ZAMM-Z. Angew. Math. Mech. 72, T537-T539.

Ulewicz, R., Jelonek, D., Mazur, M., 2016, Implementation of logic flow in planning and production control. Management and Production Engineering Review 7, 89-94.

Ulewicz, R., Selejdak, J. Borkowski, S., Jagusiak-Kocik, M., 2013. Process management in the cast iron foundry. Metal 2013: 22nd International Conference on Metallurgy and Materials. TANGER Ltd 1926-1931.

Vandersluis, E., Ravindran, C., 2018. Relationships Between Solidification Parameters in A319 Aluminum Alloy. Journal of Materials Engineering and Performance 27(3), 1109-1121.

Vaněček, D. - Sokovic, M. - Mádl, J., 2003. Selected Aspects of the Surface Integrity of Aluminium Alloy in High Speed Machining - Microhardness Variations and Surface Roughness. Journal of Mechanical Engineering - Strojniški Vestnik. 49(2), 111-115.

Villars, P., Prince, A., Okamoto, H., 1995, Al-Cu-Si, Handbook of Ternary Alloy Phase Diagrams, ASM International, Materials Park, OH, 3, p 3331-3351.

Vitalii, B., Dudek, A., 2017. Evaluation of composite epoxy resin applicability for concrete coatings. Composites Theory and Practice 17(4), 221-225.

Wojnar, L., Gadek-Moszczak, A., PIETRASZEK, J., 2019. On the role of histomorphometric (stereological) microstructure parameters in the prediction of vertebrae compression strength. Image Analysis and Stereology 38, 63-73.

Wołczyński, W., Sypien, A., Tarasek, A., Bydałek, A.W., 2017. Copper Droplets Agglomeration / Coagulation In The Conditions Similar To Industrial Ones. Archives of Metallurgy And Materials 62(1), 299-306.